VOLUME 123, NUMBER 25
JUNE 27, 2001

JOURNAL OF THE AMERICAN CHEMICAL SOCIETY

Cryoreduction of Methyl-Coenzyme M Reductase: EPR Characterization of Forms, MCR_{ox1} and MCR_{red1}

Joshua Telser,[†,‡] Roman Davydov,[†] Yih-Chern Horng,[§] Stephen W. Ragsdale,*[,§] and Brian M. Hoffman*[,†]

Contribution from the Department of Chemistry, Northwestern University, Evanston, Illinois 60208-3113, and Department of Biochemistry, Beadle Center, University of Nebraska, Lincoln, Nebraska 68588-0664

Received February 19, 2001

Abstract: Methyl-coenzyme M reductase (MCR) catalyzes the formation of methyl-coenzyme M (CH_3S-$CH_2CH_2SO_3$) from methane. The active site is a nickel tetrahydrocorphinoid cofactor, factor 430, which in inactive form contains EPR-silent Ni(II). Two such forms, denoted MCR_{silent} and $MCR_{ox1-silent}$, were previously structurally characterized by X-ray crystallography. We describe here the cryoreduction of both of these MCR forms by γ-irradiation at 77 K, which yields reduced protein maintaining the structure of the oxidized starting material. Cryoreduction of MCR_{silent} yields an EPR signal that strongly resembles that of MCR_{red1}, the active form of MCR; and stepwise annealing to 260−270 K leads to formation of MCR_{red1}. Cryoreduction of $MCR_{ox1-silent}$ solutions shows that our preparative method for this state yields enzyme that contains two major forms. One behaves similarly to MCR_{silent}, as shown by the observation that both of these forms give essentially the same redlike EPR signals upon cryoreduction, both of which give MCR_{red1} upon annealing. The other form is assigned to the crystallographically characterized $MCR_{ox1-silent}$ and directly gives MCR_{ox1} upon cryoreduction. X-band spectra of these cryoreduced samples, and of conventionally prepared MCR_{red1} and MCR_{ox1}, all show resolved hyperfine splitting from four equivalent nitrogen ligands with coupling constants in agreement with those determined in previous EPR studies and from ^{14}N ENDOR of MCR_{red1} and MCR_{ox1}. These experiments have confirmed that all EPR-visible forms of MCR contain Ni(I) and for the first time generated in vitro the EPR-visible, enzymatically active MCR_{red1} and the activate-able "ready" MCR_{ox1} from "silent" precursors. Because the solution Ni(II) species we assign as $MCR_{ox1-silent}$ gives as its primary cryoreduction product the Ni(I) state MCR_{ox1}, previous crystallographic data on $MCR_{ox1-silent}$ allow us to identify the exogenous axial ligand in MCR_{ox1} as the thiolate from CoM; the cryoreduction experiments further allow us to propose possible axial ligands in MCR_{red1}. The availability of model compounds for MCR_{red1} and MCR_{ox1} also is discussed.

Introduction

Methyl-coenzyme M reductase (MCR)[1] catalyzes the final step of methane formation by methanogenic archaea,[2] most notably *Methanothermobacter marburgensis* (*Mtm*). Formerly known as *Methanobacterium thermoautotrophicum* strain Marburg, this organism was recently reclassified.[3] The reaction involves what is formally a two-electron reduction of C_1, specifically the reaction of 2-(methylthio)ethanesulfonic acid (methyl-coenzyme M, CH_3S-CoM) with *N*-7-mercaptoheptanoylthreonine phosphate (HTP-SH, coenzyme B, CoB-SH) to yield methane and the mixed disulfide, CoM−S−S-CoB, as shown in Scheme 1.

[†] Northwestern University.
[‡] Permanent address: Chemistry Program, Roosevelt University, Chicago, IL 60605.
[§] University of Nebraska.

10.1021/ja010428d CCC: $20.00
Published on Web 05/30/2001

Scheme 1

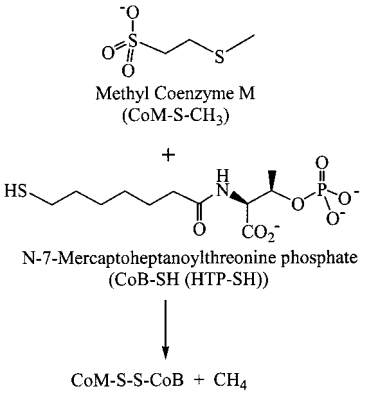

Chart 1

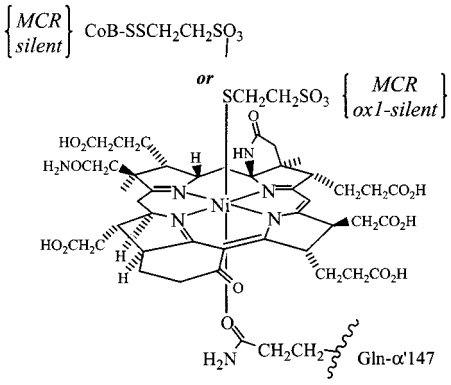

MCR contains an unusual nickel tetrahydrocorphinoid cofactor, factor 430 (F_{430}, Chart 1), which is the site of enzyme action, presumably due to the redox activity and coordinative lability of the nickel ion. High-resolution crystal structures of two different inactive states of the enzyme, denoted MCR_{silent} and $MCR_{ox1-silent}$, have been determined recently.[4] These inactive forms contain Ni(II) and are so-called because they are "EPR-silent" using conventional (X-band or Q-band (35 GHz)) spectrometers.[5] The Ni(II) ions in MCR_{silent} and $MCR_{ox1-silent}$ each have one endogenous and one exogenous ligand. In both cases, the endogenous, lower "proximal" ligand is the side-chain oxygen of Gln-α147 (see Chart 1).[4] In MCR_{silent}, the exogenous, upper "distal" ligand is a sulfonate oxygen of CoB−SS−CoM,[4] while in $MCR_{ox1-silent}$ this ligand is the thiol(ate) group of CoM-S(H).[4]

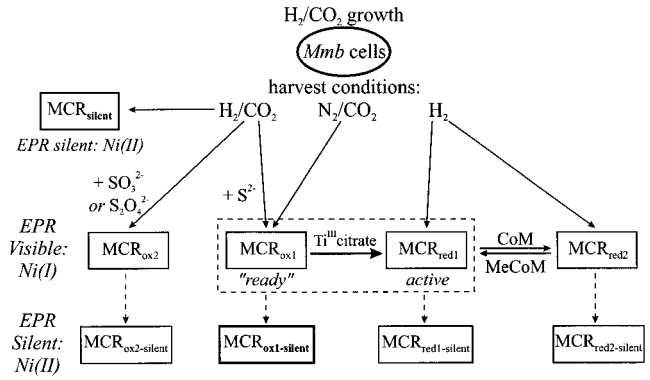

Figure 1. Diagram showing the interconversion among various *Mtm* MCR species, based largely on the work from Thauer's laboratory[2] and on findings by Becker and Ragsdale.[8] The assignment of EPR-visible forms of MCR to Ni(I) is based on the work described herein and on previous work.[15] The dashed arrows indicate the conversion over time, even under anaerobic conditions, of EPR-visible forms of MCR to EPR-silent forms.

As summarized in Figure 1, the structurally characterized forms of MCR are but two of many. MCR_{silent} (the label denotes that it is "EPR-silent," as are all forms labeled "silent") is the enzyme form that is isolated when the cells are harvested from the normal gas-phase growth medium (80% H_2/20% CO_2). $MCR_{ox1-silent}$ is not directly isolated but forms over time under anaerobic conditions from the EPR-visible MCR_{ox1}, which itself is formed when the gas medium is made less reducing (80% N_2/20% CO_2),[2,6,7] *or* when the normal gas medium is used, but the growing cells are treated with sodium sulfide.[8] Preliminary X-ray studies[9] confirm that crystals obtained from $MCR_{ox1-silent}$ solutions prepared via the latter method[8] exhibit the same Ni(II) coordination as found previously for $MCR_{ox1-silent}$ prepared by the former procedure.[2,4,6]

Perhaps the most important enzyme form is the EPR-visible MCR_{red1}, which has been correlated with enzyme activity. MCR_{red1} results when the gas medium is made the most reducing (100% H_2),[2,6] but it converts over time to another EPR-silent species, $MCR_{red1-silent}$.

None of these "silent" forms can be reconverted to its progenitor EPR-visible form in vitro. However, MCR_{ox1} can be quantitatively converted to the enzymatically and EPR-visible MCR_{red1} form by addition of Ti(III) citrate in vitro.[10] Hence, MCR_{ox1} may be considered an activateable, or "ready" form of the enzyme.

The question as to the formal oxidation state of Ni in the EPR-visible forms of MCR is a thorny one. MCR_{red1} is unambiguously assigned to Ni(I) based on its UV−visible and EPR spectral correspondence with isolated $Ni^{I}F_{430}$.[2,11,12] The EPR spectra of MCR_{red1}, $Ni^{I}F_{430}$, and complexes of the $3d^9$ ions Cu(II) or Ni(I) in tetragonally elongated or square planar geometry are roughly axial with $g_{||} \approx (2.2-2.3) > g_{\perp} \sim 2.05 \gtrsim g_e$, which result from unpaired electron occupancy of the $d_{x^2-y^2}$

(1) Abbreviations used: CoM, coenzyme M, 2-(methylthio)-ethanesulfonic acid; CW, continuous wave; ENDOR, electron nuclear double resonance; F_{430}, nickel tetrapyrrole pentacarboxylic acid cofactor; $F_{430}Me_5$, nickel tetrapyrrole pentamethyl ester cofactor; hwhm, half width at half-maximum; MCD, magnetic circular dichroism; MCR, methyl coenzyme M reductase; *Mtm*, *Methanothermobacter marburgensis*; OEiBC, octaethylisobacteriochlorin; THF, tetrahydrofuran.

(2) Thauer, R. K. *Microbiology* **1998**, *144*, 2377−2406.

(3) Wasserfallen, A.; Nolling, J.; Pfister, P.; Reeve, J.; De Macario, E. C. *Int. J. Syst. Evol. Microbiol.* **2000**, *50*, 43−53.

(4) Ermler, U.; Grabarse, W.; Shima, S.; Goubeaud, M.; Thauer, R. K. *Science* **1997**, *278*, 1457−1462.

(5) This "silence" is not due to the cofactor's Ni(II) ion being in a square planar geometry with $S = 0$, as is often the case, e.g., in Ni(II) porphyrins. (Renner, M. W.; Furenlid, L. R.; Barkigia, K. M.; Forman, A.; Shim, H. K.; Simpson, D. J.; Smith, K. M.; Fajer, J. *J. Am. Chem. Soc.* **1991**, *113*, 6891−6896.) Rather, it is the consequence of the $S = 1$ Ni(II) ion existing in a tetragonally elongated octahedral geometry that leads to large axial zero-field splitting: $D \approx +9$ cm^{-1}, as determined by MCD for MCR_{silent}. (Cheesman, M. R.; Ankel-Fuchs, D.; Thauer, R. K.; Thomson, A. J. *Biochem. J.* **1989**, *260*, 613−616. Hamilton, C. L.; Scott, R. A.; Johnson, M. K. *J. Biol. Chem.* **1989**, *264*, 11605−11613). Thus, no EPR transitions fall within the field/frequency range of conventional spectrometers.

(6) Albracht, S. P. J.; Ankel-Fuchs, D.; Böcher, R.; Ellermann, J.; Moll, J.; van der Zwaan, J. W.; Thauer, R. K. *Biochim. Biophys. Acta* **1988**, *941*, 86−102.

(7) Albracht, S. P. J.; Ankel-Fuchs, D.; van der Zwaan, J. W.; Fontijn, R. D.; Thauer, R. K. *Biochim. Biophys. Acta* **1986**, *870*, 50−57.

(8) Becker, D. F.; Ragsdale, S. W. *Biochemistry* **1998**, *37*, 2369−2647.

(9) Thauer, R. K., personal communication.

(10) Goubeaud, M.; Schreiner, G.; Thauer, R. *Eur. J. Biochem.* **1997**, *243*, 110−114.

(11) Holliger, C.; Pierik, A. J.; Reijerse, E. J.; Hagen, W. R. *J. Am. Chem. Soc.* **1993**, *115*, 5651−5656.

(12) Telser, J. In *Structure and Bonding*; Williams, R. J. P., Ed.; Springer Verlag: Heidelberg, 1998; Vol. 91, pp 31−63.

Table 1. **g** Tensors for EPR−Visible MCR States and Models Determined by 35-GHz EPR at 2 K

	$g_{1\,(max)}$[b]	$g_{2\,(mid)}$[b]	$g_{3\,(min)}$[b]
MCR (and model) species:[a] redlike			
$Ni^{I}F_{430}$	2.244(2)	2.063(2)	2.063(2)
Ni^{I}OEiBC	2.204(1)	2.080(2)	2.063(2)
MCR_{red1}[c]	2.245(5)	2.065(5)	2.057(5)
MCR_{red1}, from MCR_{silent}[d]	2.240(1)	2.060(2)	2.052(2)
MCR_{red1}, from $MCR_{ox1-silent}$[e]	2.243(2)	2.065(5)	2.060(5)
$[MCR_{silent}R]_{77}$[f]	[2.305(5), 2.285(5)]	2.088(3)	2.073(3)
$[MCR_{ox1-silent}R]_{77}$[g]	[2.31(1), 2.29(1)]	[2.11(1), 2.08(1)]	[2.11(1), 2.08(1)]
MCR species: oxlike			
MCR_{ox1}[h]	2.229(2)	2.165(2)	2.148(2)
MCR_{ox2}	2.227(2)	2.140(5)	2.125(5)
MCR_{ox1}, from $MCR_{ox1-silent}$[i]	2.229(1)	2.165(1)	2.148(2)
$[MCR_{silent}O]_{77}$[j]	2.195(5)	2.128(2)	2.118(2)

[a] Values for EPR-visible MCR species generated at ambient temperature are taken from Telser et al.[15] Values for the model compounds $Ni^{I}F_{430}$ and Ni^{I}OEiBC are taken from Telser et al.[38] Values obtained by other workers, using X-band EPR, on the above [11,35,36] are in good agreement with the 35-GHz data. These and values for other Ni(I) complexes[42] are summarized by Telser.[12] All samples were in aqueous solution, except for Ni^{I}OEiBC, which was in 2-Me-THF solution. [b] Values in parentheses are uncertainties; values in brackets represent groupings of similar g values. [c] The values reported for conventionally (biochemically) prepared MCR_{red1} are for the specific sample shown; different preparations and conditions (e.g., amount of glassing agent) lead to slight parameter variation as given by the uncertainties, which are larger than those for the actual spectrum. Simulation used Gaussian single-crystal line width (hwhm) of $W_{iso} = 90$ MHz. Simulation of X-band spectra (see Figure 4) required: $\mathbf{g} = [2.242, 2.065, 2.058]$, four identical nitrogen ligands with $a_{iso}(^{14}N) = 30$ MHz, single-crystal Gaussian line widths (hwhm), $W_{x,y,z} = [40, 13, 13]$ MHz. [d] MCR_{red1} generated by cryoreduction of MCR_{silent} (to form $[MCR_{silent}R]_{77}$) followed by annealing to fluid solution (262 K). Simulation used $W_{x,y,z} = [85, 80, 75]$ MHz. Simulation of X-band spectra (see Figure 4) required the following: $\mathbf{g} = [2.245, 2.065, 2.065]$; four identical nitrogen ligands with $a_{iso}(^{14}N) = 30$ MHz; $W_{x,y,z} = [20, 16, 16]$ MHz. [e] MCR_{red1} generated by cryoreduction of $MCR_{ox1-silent}$ (to form $[MCR_{ox1-silent}R]_{77}$) followed by annealing to fluid solution (267 K). Simulation used $W_{x,y,z} = [90, 80, 80]$ MHz. Simulation of X-band spectra (see Figure 4) required the following: $\mathbf{g} = [2.24(1), 2.064, 2.064]$; four identical nitrogen ligands with $a_{iso}(^{14}N) = 28$ MHz; $W_{iso} = 15$ MHz. [f] Species generated by cryoreduction of MCR_{silent}. The values in brackets represent two species with differing values for g_z ($g_z \equiv g_{||} \equiv g_{1(max)}$), but the same for g_x and g_y ($g_y \equiv g_{2(mid)}$, $g_x \equiv g_{3(min)}$). Simulation used $W_{x,y,z} = [(70, 160), 70, 80)]$ MHz; any variation in g_x or g_y between the two components must therefore be less than ~0.005 (~80 MHz). [g] Species generated by cryoreduction of $MCR_{ox1-silent}$. No simulations or specific correspondence among g values is possible due to spectral complexity. There are also very weak features with $g > 2.31$. [h] Conventionally (biochemically) prepared MCR_{ox1}. Simulation used $W_{iso} = 75$ MHz. Simulation of X-band spectra (see Figure 4) required the following: $\mathbf{g} = [2.230, 2.167, 2.153]$, and four identical nitrogen ligands with $A(^{14}N) = [27, 30, 30]$ MHz, $W_{x,y,z} = [13, 15, 13]$ MHz. [i] MCR_{ox1} generated by cryoreduction of $MCR_{ox1-silent}$ followed by annealing to fluid solution (267 K) Simulation used $W_{x,y,z} = [70, 70, 75]$ MHz. Simulation of X-band spectra (see Figure 3) required the following: $\mathbf{g} = [2.231, 2.155, 2.155]$; four identical nitrogen ligands with $a_{iso}(^{14}N) = 28$ MHz; $W_{x,y,z} = [13, 15, 15]$ MHz. Initial cryoreduction yields a major signal with $\mathbf{g} = [2.23(1), 2.17(1), 2.15(1)]$, which remains unchanged during annealing and is MCR_{ox1}. Initial cryoreduction also yields a minor signal with $\mathbf{g} \approx [2.20(1), 2.14(1),$ not obs] that diminishes greatly upon annealing. There is an additional feature at $g \approx 2.24$, but this is due to initially generated MCR_{red1}. [j] This signal is of very weak intensity; it diminishes upon annealing and is absent by 262 K. It may be related to the minor oxlike signal described above for $MCR_{ox1-silent}$.

orbital.[13] In contrast, MCR_{ox1} and a related form, denoted MCR_{ox2},[2] do not exhibit EPR spectra that correspond closely to the above systems, in that although $g_{||} \approx 2.23$, they exhibit an unusually large value $g_{\perp} \approx 2.15$ (EPR data for major forms of MCR are summarized in Table 1). Nonetheless, the EPR spectra of neither MCR_{ox1} nor MCR_{ox2} correspond to that of isolated $Ni^{III}F_{430}Me_5$,[14] which exhibits EPR typical of the $3d^7$ ions Co(II) or Ni(III) in tetragonally elongated geometry, with unpaired electron occupancy of the d_{z^2} orbital. Such spectra are roughly axial with $g_{\perp} \approx (2.2-2.3) > g_{||} \approx g_e$.[13]

We have proposed that all EPR-visible forms of MCR contain Ni in the (I) formal oxidation state[15] and that the conversion to EPR-silent forms results from slow oxidation of Ni(I) to Ni(II), even under nominally anaerobic conditions. This proposal was based on consideration of spectroscopic factors, particularly the ^{14}N ENDOR similarity among $MCR_{ox1,\ 2}$ and MCR_{red1} and authentic Ni(I) model compounds, consideration of recent biochemical evidence,[8] and the wealth of data on tetraaza-macrocyclic compounds of nickel.[12,15]

This assignment was in some cases contrary to prior expectations, as indicated by the label "ox" for several EPR-visible forms. Consequently, in the present study, we have sought additional experimental evidence to test this assignment. In addition, we address other important questions. Can one find a way to convert the enzymatically inactive and EPR-silent forms of MCR to enzymatically active (MCR_{red1}) or activateable ("ready", MCR_{ox1}) forms? What is the structural basis for the difference among EPR signals for the different Ni(I) MCR forms, and in particular, what are the axial ligands to Ni in MCR_{ox1} and MCR_{red1}? Taking MCR_{ox1} and MCR_{red1} both as containing Ni(I), then what is the role of the presumed reductant Ti(III) citrate in the conversion of the former to the latter?

The present study addresses these questions, by "giving voice" to the thus far structurally characterized but EPR-silent forms of MCR. These are converted to EPR-visible states through cryoreduction. In this technique, γ-irradiation of solutions frozen at cryogenic temperatures (~77 K) generates mobile electrons from the matrix that can reduce redox-active sites generating an EPR-visible reduced enzyme form retaining the structure of the parent oxidized species. Multiple, reduced "daughter" species can be simultaneously produced, which correspond to the presence in solution of multiple "parent" conformations. Such species generally do not interconvert at 77 K. These primary products of reduction can then be annealed at progressively higher temperatures to allow reorganization in response to the reduction to occur in a stepwise, controlled manner. This cryoreduction technique has been successfully applied to a wide variety of metalloproteins, such as heme proteins[16,17] diiron oxo proteins,[18−21] and iron−sulfur proteins.[22−24]

(13) Maki, A. H.; Edelstein, N.; Davison, A.; Holm, R. H. *J. Am. Chem. Soc.* **1964**, *86*, 4580−4587.
(14) Jaun, B. *Helv. Chim. Acta* **1990**, *73*, 2209−2216.
(15) Telser, J.; Horng, Y.-C.; Becker, D. F.; Hoffman, B. M.; Ragsdale, S. W. *J. Am. Chem. Soc.* **2000**, *122*, 182−183.
(16) Davydov, R. M.; Yoshida, T.; Ikeda-Saito, M.; Hoffman, B. M. *J. Am. Chem. Soc.* **1999**, *121*, 10656−10657.
(17) Davydov, R.; Macdonald, I. D. G.; Makris, T. M.; Sligar, S. G.; Hoffman, B. M. *J. Am. Chem. Soc.* **1999**, *121*, 10654−10655.
(18) Davydov, R.; Valentine, A. M.; Komar-Panicucci, S.; Hoffman, B. M.; Lippard, S. J. *Biochemistry* **1999**, *38*, 4188−4197.

We present here X- and Q-band EPR studies on solutions of MCR_{silent} and $MCR_{ox1-silent}$ that have been cryoreduced at 77 K. These studies provide corroborative evidence for the Ni(I) oxidation assignment made previously.[15] The correlation we observe between the primary, Ni(I), "daughter" species generated by cyroreduction and their EPR-silent, Ni(II), "parent" species allows us to use prior crystallographic data[4] to propose an identification of the axial ligands of MCR_{ox1} and infer the possible candidates for these ligands in MCR_{red1}.

Experimental Section

Preparation of $MCR_{ox1-silent}$ and MCR_{silent} Samples. *Methanothermobacter marburgensis* (*Mtm*) (formerly known as *Mb. thermoautotrophicum* strain Marburg[3]) was cultured on $H_2/CO_2/H_2S$ (80%/20%/0.1%) at 65 °C in a 14-L New Brunswick fermentor.[10,25] Media were prepared as previously described.[25] For the preparation of MCR_{silent}, *Mtm* cells were harvested at the end of the exponential growth phase ($A_{578} \sim 3.0$). For the generation of the MCR_{ox1} state, 20 mM sodium sulfide (final concentrated) was added directly to the growing cells at late log phase ($A_{578} \sim 3.0$) and incubated for 15 min at 65 °C. The culture was then cooled to 25 °C within 30 min and harvested anaerobically.[8] MCR_{ox1} and MCR_{silent} were purified as described.[10] $MCR_{ox1-silent}$ was prepared [26] by exposing purified MCR_{ox1} (0.54 spins/mol, specific activity 8.0 units/mg) to air at room temperature overnight. The completed formation of $MCR_{ox1-silent}$ was checked by EPR (below 0.005 spins/mol MCR_{ox1}). MCR samples used in irradiation experiments contained 10% (v/v) glycerol, 50 mM Tris-HCl at pH 7.6. $MCR_{ox1-silent}$ and MCR_{silent} were concentrated to 1.03 and 1.8 mM, respectively, under argon (that had been passed through an Oxisorb column) pressure in a 10-mL Omegacell (Filtron) with a 30-kDa molecular mass cutoff. Protein concentrations were determined by the Bradford method using the Bio-Rad reagent (Bio-Rad) and bovine serum albumin as a standard.[27] F_{430} content was estimated using an extinction coefficient of 22 000 cm^{-1} M^{-1} at 420 nm.[28]

EPR/ENDOR Spectroscopy. X-band (~9 GHz) CW EPR spectra at 77 K were recorded on a modified Varian E-9 spectrometer (Northwestern) or on a Bruker ESP 300E (Nebraska). CW "Q"-band (35-GHz) EPR/ENDOR spectra were recorded on a modified Varian E-109 spectrometer. All CW Q-band EPR/ENDOR spectra were recorded at 2 K and in dispersion mode, under "rapid-passage" conditions, which gives an absorption line shape.[29,30] All X-band spectra were recorded using conventional absorption mode, giving a first-derivative line shape, as normally reported. Quantitation of X-band EPR spectra employed $Cu^{II}EDTA$ as a signal intensity standard, which is a $3d^9$ $S = {}^1/_2$ complex electronically similar to the Ni^IF_{430} center in EPR-visible MCR. Quantitation of 35-GHz spectra is not as reliable because of the relaxation effects in rapid-passage EPR. Computer simulation of EPR spectra used the program QPOWA.[31]

Cryoreduction Procedure. The procedure is the same as that described previously in more detail.[18] MCR samples in fused silica EPR tubes immersed in liquid nitrogen were exposed to ^{60}Co γ-irradiation, typically for ~12 h (3.5-Mrad dose). MCR samples were checked by EPR immediately prior to irradiation and none showed signals at either 77 (X-band) or 2 K (35 GHz). Annealing at multiple temperatures over the range 77−270 K was performed by placing the EPR tube in the appropriate slush bath (e.g., *n*-pentane/$N_{2(l)}$) typically for 60 s and then refreezing in liquid nitrogen. The bath temperature was determined by a thermocouple. Several replicates of each sample were investigated, and all gave essentially identical EPR results, both initially and after annealing. Cryoreduced MCR samples maintained at 77 K (i.e., never annealed) showed no change by EPR over a period of months, indicating both the stability of the cryoreduction products and the absence of any interconversion at 77 K.

As shown previously,[16−20,22] γ-irradiation at 77 K of metalloprotein frozen solutions yields an intense EPR signal at $g = 2.00$ that corresponds to organic radicals that are normally of no interest. Such signals are seen in the irradiated MCR-silent samples and are truncated in the reported spectra. Additionally, γ-irradiation at 77 K produces hydrogen atoms within the fused silica tubes, which give the characteristic hyperfine doublet ($A(^1H\bullet) = 1420$ MHz $= 50.7$ mT), as seen in Figure S1 for MCR_{silent} (Supporting Information; the low-field partner of the H atom doublet is seen in Figure S3 for $MCR_{ox1-silent}$). As seen in all cases, as the annealing temperature is raised, radical recombination occurs and the signal at $g = 2.00$ due to organic radicals decreases significantly.

Results

The present data will be discussed in terms of the two classes of EPR spectra characteristic of EPR-visible MCR states: those typified by MCR_{ox1} ("oxlike") and those by MCR_{red1} ("redlike"). All have axial (or nearly so) **g** tensors with $g_{||} > g_\perp > g_e$, characteristic of a $d_{x^2-y^2}{}^1$ ground state.[13] Oxlike spectra have $g_{||} \approx 2.25$ and an anomalously large $g_\perp \approx 2.16$; redlike spectra have only a slightly larger $g_{||} \approx 2.3$ but a more common value $g_\perp \approx 2.05$.

As described in the Experimental Section, spectra at X-band were recorded at 77 K in conventional absorption mode, giving first-derivative line shapes, while Q-band spectra were recorded at 2 K in dispersion mode, giving absorption line shapes. In describing the species formed during cryoreduction, we focus initially on Q-band spectra, which provide better dispersion of *g* values. These are digitally converted to derivative spectra for presentation in a more familiar appearance as shown in Figures 2 and 3, respectively, for MCR_{silent} and $MCR_{ox1-silent}$. The Supporting Information shows the original (absorption line shape) 35-GHz spectra for MCR_{silent} in Figure S1 and for $MCR_{ox1-silent}$ in Figure S2; corresponding X-band spectra are shown in Figures S3 and S4, respectively, for MCR_{silent} and $MCR_{ox1-silent}$.

Cryoreduction of MCR_{silent}. Figure 2 presents the 2 K Q-band EPR spectrum ($g > 2.03$) of MCR_{silent} that has been cryoreduced at 77 K, as well as spectra taken while the sample is progressively annealed at higher temperatures and a spectrum of MCR_{red1} generated by standard procedures.[8] The major species generated by cryoreduction of MCR_{silent} at 77 K exhibits an axial EPR signal that resembles that of MCR_{red1}, with $g_{||} \approx 2.3$ and $g_\perp \approx 2.09$ (the perpendicular feature is distorted by overlap with signals from organic radicals). Hence, this species is denoted $[MCR_{silent}R]_{77}$. Looking at $g_{||}$ in Figure 2 (77 K), the spectrum exhibits several minor features, which indicates that MCR_{silent}, the parent state, is somewhat heterogeneous.

(19) Davydov, R.; Sahlin, M.; Kuprin, S.; Graslund, A.; Ehrenberg, A. *Biochemistry* **1996**, *35*, 5571−5576.
(20) Davydov, A.; Davydov, R.; Graslund, A.; Lipscomb, J.; Anderson, K. K. *J. Biol. Chem.* **1997**, *272*, 7022−7026.
(21) Davydov, R.; Kuprin, S.; Graslund, A.; Ehrenberg, A. *J. Am. Chem. Soc.* **1994**, *116*, 11120−11128.
(22) Dikanov, S. A.; Davydov, R. M.; Xun, L.; Bowman, M. K. *J. Magn. Reson.* **1996**, *112*, 289−294.
(23) Telser, J.; Davydov, R.; Kim, C. H.; Adams, M. W. W.; Hoffman, B. M. *Inorg. Chem.* **1999**, *38*, 3550−3553.
(24) Yoo, S. J.; Angove, H. C.; Burgess, B. K.; Münck, E.; Peterson, J. *J. Am. Chem. Soc.* **1998**, *120*, 9704−9705.
(25) Schönheit, P.; Moll, J.; Thauer, R. K. *Arch. Microbiol.* **1980**, *127*, 59−65.
(26) Shima, S.; Goubeaud, M.; Vinzenz, D.; Thauer, R. K.; Ermler, U. *J. Biochem.* **1997**, *121*, 829−830.
(27) Bradford, M. M. *Anal. Biochem.* **1976**, *72*, 248−254.
(28) Pfaltz, A.; Juan, B.; Fassler, A.; Eschenmoser, A.; Jaenchen, R.; Gilles, H. H.; Diekart, G.; Thauer, R. K. *Helv. Chim. Acta* **1982**, *65*, 828−865.
(29) Hoffman, B. M.; Gurbiel, R. J.; Werst, M. M.; Sivaraja, M. In *Advanced EPR. Applications in Biology and Biochemistry*; Hoff, A. J., Ed.; Elsevier: Amsterdam, 1989; pp 541−591.
(30) Hoffman, B. M.; DeRose, V. J.; Doan, P. E.; Gurbiel, R. J.; Houseman, A. L. P.; Telser, J. In *Biological Magnetic Resonance*; Berliner, L. J., Reuben, J., Eds.; Plenum Press: New York, 1993; Vol. 13, pp 151−218.
(31) Belford, R. L.; Nilges, M. J. In *EPR Symposium, 21st Rocky Mountain Conference*: Denver, CO, August 1979.

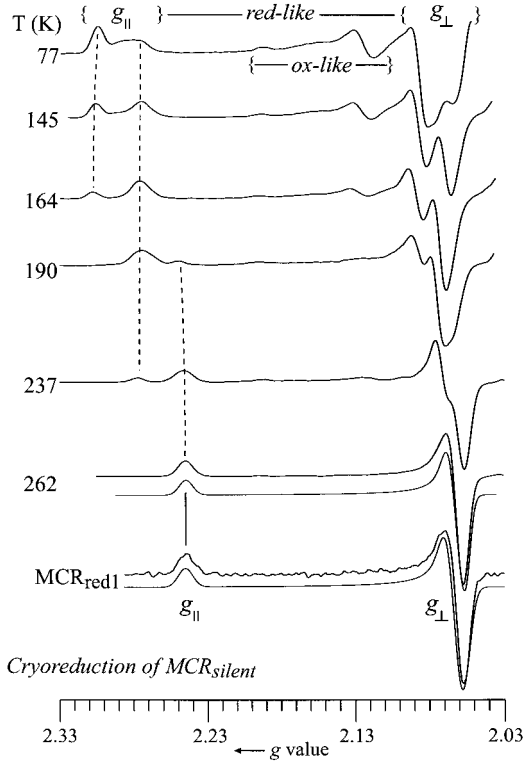

Figure 2. Q-Band EPR spectra of 77 K cryoreduced MCR$_{silent}$ as a function of annealing temperature. The annealing temperature is given for each spectrum. The abscissa is in g value and the spectra are presented as digital first derivatives, to allow better visualization of the spectral changes as a function of annealing temperature. A simulation is shown for sample annealed at 262 K. Also included is a spectrum of conventionally (biochemically) prepared MCR$_{red1}$ with a simulation. Experimental conditions for cryoreduced samples: protein concentration, 1.8 mM; 50 mM Tris-HCl, pH 7.6, plus 10% (v/v) glycerol; temperature, 2 K; microwave frequency, 77−237 K 35.209 GHz, 262 K 35.220 GHz; microwave power, 8 μW (44 dB); 100-kHz field modulation amplitude, 0.13 mT; time constant, 128 ms; 4 scans. Experimental conditions for biochemically prepared MCR$_{red1}$: microwave frequency, 34.945 GHz; microwave power, 20 μW; 100-kHz field modulation amplitude, 0.1 mT; time constant, 64 ms; 1 scan. Guidelines are provided to track the various features as described in the text. Simulation parameters: 262 K $\mathbf{g} = [2.240, 2.060, 2.052]$; single-crystal Gaussian line widths (hwhm), $W_{x,y,z} = [85, 80, 75]$ MHz; authentic MCR$_{red1}$ $\mathbf{g} = [2.245, 2.065, 2.057]$; $W_{iso} = 90$ MHz.

Computer simulations reproduce quite well the experimental spectrum of [MCR$_{silent}$R]$_{77}$ using a superposition of signals from two similar Ni(I) centers, differing only in g_1.[32] Table 1 collects EPR data for [MCR$_{silent}$R]$_{77}$ and other systems of interest.

Stepwise annealing of a cryoreduced MCR state allows its conformation to relax from that of the parent Ni(II) species, eventually reaching the equilibrium "relaxed" structure of the Ni(I) state. Upon annealing cryoreduced MCR$_{silent}$, the $g_{||}$ region undergoes the changes highlighted by the guidelines in Figure 2, with full annealing (262 K) yielding the single "relaxed" species, MCR$_{red1}$, as is shown by comparing its spectrum to that of MCR$_{red1}$ generated by conventional biochemical methods (see Table 1). This is the first reported conversion in vitro of

(32) Also present in Figure 2 (77 K) is a minor signal, with an intensity of ~10% that of [MCR$_{silent}$R]$_{77}$. This species has g values that are oxlike, and we therefore denote it [MCR$_{silent}$O]$_{77}$. Simulation shows that its **g** tensor is perhaps closest to that of MCR$_{ox2}$ (see Table 1). This conclusion suggests that frozen solution samples of MCR$_{silent}$ may contain minority components of a "silent-ox" species, which might even be MCR$_{ox2-silent}$. During the annealing process, [MCR$_{silent}$O]$_{77}$ progressively decreases in intensity and is totally absent by 262 K.

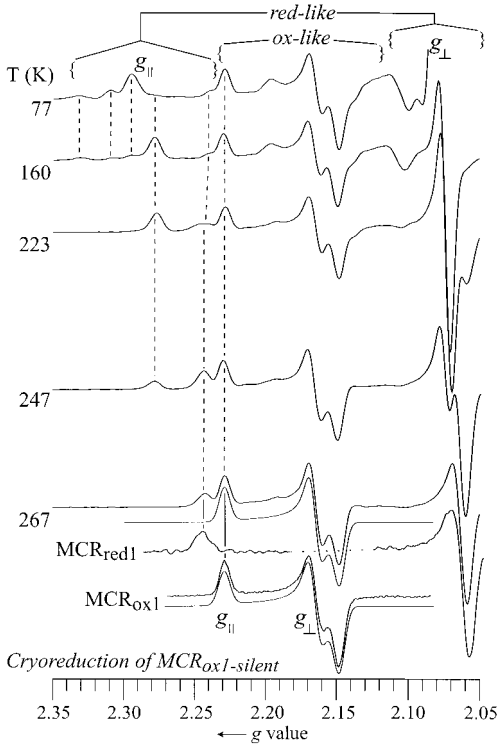

Figure 3. Q-Band EPR spectra of 77 K cryoreduced MCR$_{ox1-silent}$ as a function of annealing temperature. The annealing temperature is given for each spectrum. The abscissa is in g value and the spectra are presented as digital first derivatives. A simulation is shown for sample annealed at 267 K. Also included are spectra of conventionally (biochemically) prepared MCR$_{ox1}$ with a simulation and of MCR$_{red1}$. Experimental conditions: as in Figure 2, except for protein concentration (1.03 mM) and microwave frequency 77 and 160 K, 35.143 GHz; 223 and 247 K, 35.172 GHz; 267 K, 35.166 GHz; MCR$_{ox1}$, 34.968 GHz. Guidelines are provided to track the various features as described in the text. Simulation parameters: 267 K, $\mathbf{g} = [2.229, 2.165, 2.148]$; $W_{x,y,z} = [70, 70, 75]$ MHz; the remaining "redlike" features, which for clarity have no simulation shown, can be simulated by $\mathbf{g} = [2.243, 2.065, 2.060]$, $W_{x,y,z} = [90, 80, 80]$ MHz; for authentic MCR$_{ox1}$ $\mathbf{g} = [2.229, 2.166, 2.148]$; $W_{iso} = 75$ MHz.

MCR$_{silent}$ to the enzymatically active MCR$_{red1}$. On the basis of spin quantitation of X-band spectra, the applied γ-irradiation dose (~3.5 Mrad) yields a net conversion of 15 ± 5% of MCR$_{silent}$ into MCR$_{red1}$.

Cryoreduction of MCR$_{ox1-silent}$. Cryoreduction of MCR$_{ox1-silent}$ produces *both* oxlike and redlike Q-band EPR signals with comparable intensity (Figure 3). Considering the redlike features, the $g_{||}$ region comprises a major component with $g_{||} = 2.30$ and $g_{\perp} \approx 2.08$ (there are minor components nearby at $g_{||} \approx 2.31$ and 2.33 and $g_{\perp} \approx 2.11$). This redlike spectrum is denoted [MCR$_{ox1-silent}$R]$_{77}$ and is similar, although not identical to [MCR$_{silent}$R]$_{77}$ (see Table 1). During annealing, the redlike signals progressively shift and coalesce to yield a single relaxed signal (Figure 3, 267 K), that of biochemically produced MCR$_{red1}$ (see Table 1).

The other major signal produced by cryoreduction is that of MCR$_{ox1}$, with a rhombic tensor, $\mathbf{g} = [2.23(1), 2.17(1), 2.15(1)]$ (weaker features are also present that have g values that resemble those of [MCR$_{silent}$O]$_{77}$ and MCR$_{ox2}$ (see Table 1)). The MCR$_{ox1}$ signal produced by 77 K cryoreduction of the MCR$_{ox1-silent}$ solution remains unchanged throughout the annealing process.[33] The yield of relaxed Ni(I) species is again 15 ± 5%, with roughly equal amounts of MCR$_{ox1}$ and MCR$_{red1}$. This result was

(33) Its absolute intensity may decrease slightly.

obtained for several samples from independently isolated enzyme batches.

The cryoreduction spectra, with two major "daughter" signals, thus show that our preparative method for the Ni(II) parent $MCR_{ox1-silent}$ yields enzyme that contains two major forms, not only $MCR_{ox1-silent}$, but a second Ni(II) form as well. This second form must be MCR_{silent}, or a close equivalent, because the cryoreduction spectra contain a primary signal, denoted $[MCR_{ox1-silent}R]_{77}$, that is essentially the same as that generated by reduction of MCR_{silent}, $[MCR_{silent}R]_{77}$, and annealing converts both these primary products to MCR_{red1}. By elimination, we assign $MCR_{ox1-silent}$ itself as the parent of the MCR_{ox1} formed by cryoreduction.

X-Band Spectra and ^{14}N Hyperfine Splittings. The complete set of X-band EPR spectra of cryoreduced and annealed MCR, presented in the Supporting Information (in Figure S3 for MCR_{silent} and in Figure S4 for $MCR_{ox1-silent}$), show the same behavior as at Q-band, although the poorer g value dispersion makes the process more difficult to follow. However, at the lower, X-band microwave frequency, new "super" hyperfine splittings are resolved, as is often true.[34] The spectra taken of unannealed samples (77 K) exhibit such splittings, particularly for $MCR_{ox1-silent}$, but this is best resolved in the spectra of the fully annealed (relaxed) species. This is shown in Figure 4, which also includes novel (see below) X-band spectra of conventionally (biochemically) prepared MCR_{ox1} and MCR_{red1}.

The X-band spectrum in Figure 4 of MCR_{red1} prepared by cryoreduction of MCR_{silent} shows a ^{14}N hyperfine splitting pattern at $g_\perp$ that is identical to those of Ni^IF_{430} electrochemically generated from isolated cofactor in aqueous solution,[11] chemically generated $Ni^IF_{430}Me_5$,[35] and Ni^IOEiBC,[36] in organic solvents. The ^{14}N pattern is well simulated using four equivalent ^{14}N nuclei ($I = 1$) from the four pyrrole/pyrrolidine nitrogen ligands with $a_{iso}(^{14}N) = 30(2)$ MHz; simulation with fewer than four coupled nuclei is unsuccessful. This value of $a_{iso}(^{14}N)$ is in excellent agreement with those determined from resolved X-band EPR spectra for both aqueous[11] and organic solutions of Ni^IF_{430} ($Ni^IF_{430}Me_5$ in THF),[35] and Ni^IOEiBC.[36] Such resolved EPR spectra having never been reported for conventionally generated MCR_{red1}. As a result, we reinvestigated the EPR behavior of MCR_{red1} and find that it is indeed possible to obtain X-band EPR spectra of conventionally generated MCR_{red1} that also exhibit resolved ^{14}N hyperfine splitting at $g_\perp$ (Figure 4).[37] There is thus no spectroscopically significant distinction between MCR_{red1} generated by cryoreduction and by conventional biochemical methods.

The X-band EPR spectra of relaxed cryoreduced $MCR_{ox1-silent}$ show the signals from MCR_{ox1} and MCR_{red1} (Figure 4) seen at Q-band (Figure 3), but the X-band spectra of both species again show well-resolved ^{14}N hyperfine splittings. Examination of the $g_\perp$ region shows that MCR_{red1} prepared by cryoreduction of $MCR_{ox1-silent}$ has a ^{14}N pattern identical to that of MCR_{red1} prepared by cyroreduction of MCR_{silent}; the $g_{||}$ region in the former spectrum is obscured by MCR_{ox1}. MCR_{ox1} generated by cryoreduction of $MCR_{ox1-silent}$ shows beautifully resolved hyperfine splitting from four ^{14}N nuclei at *both* $g_{||}$ and $g_\perp$ (Figure 4). We had not previously obtained such spectra for conventionally prepared MCR_{ox1}; thus, we reexamined chemically prepared MCR_{ox1} and found resolved hyperfine couplings from four ^{14}N nuclei at both $g_{||}$ and $g_\perp$ (see Figure 4 and Table 1). Essentially the same EPR results for MCR_{ox1} in *Mtm* whole cells had been reported much earlier by Albracht et al.[7] Thus, conventionally generated and cryoreduction-generated MCR_{ox1} are identical.

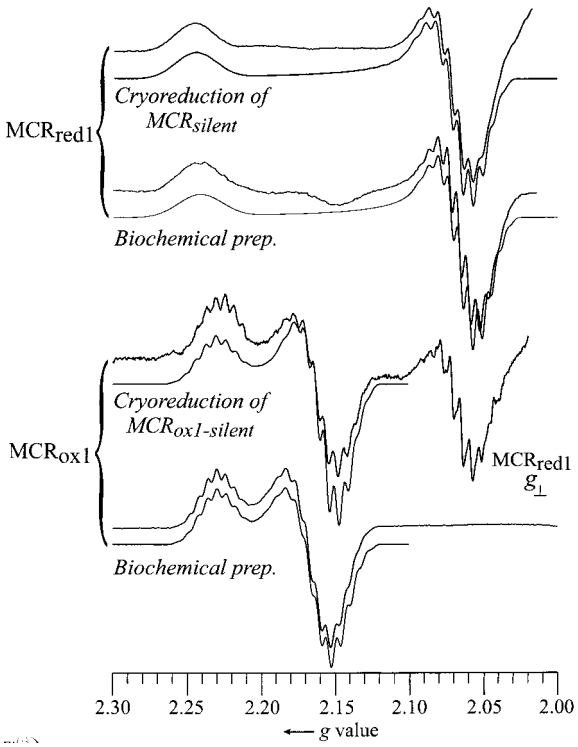

Figure 4. X-Band EPR spectra of cryoreduced, annealed MCR_{silent} and $MCR_{ox1-silent}$, together with spectra of biochemically prepared MCR_{red1} and MCR_{ox1}, with simulations for each of these. Experimental conditions: *cryoreduced* MCR_{silent}, temperature, 77 K; protein concentration, 1.0 mM (0.15 spins/mol); microwave frequency, 9.087 GHz; microwave power, 20 mW; 100-kHz field modulation amplitude, 0.5 mT; time constant, 128 ms; 4 scans. *Cryoreduced* $MCR_{ox1-silent}$, same as cryoreduced MCR_{silent} except protein concentration, 0.16 mM (0.37 spins/mol); microwave frequency, 9.450 GHz; microwave power, 8 mW; time constant, 164 ms; 10 scans. *Biochemical* MCR_{red1}, same as cryoreduced, except microwave frequency, 9.245 GHz; 100-kHz field modulation amplitude, 0.2 mT. A very small amount of MCR_{ox1} is also present, which leads to the feature at $g \approx 2.15$. *Biochemical* MCR_{ox1}, same as biochemical MCR_{red1}, except protein concentration, 0.25 mM (0.50 spins/mol); microwave frequency, 9.4744 GHz, 1 scan. Simulation parameters: *cryoreduced* MCR_{red1}, $\mathbf{g} = [2.245, 2.065, 2.065]$; four identical nitrogen ligands with $a_{iso}(^{14}N) = 30$ MHz, single-crystal Gaussian line widths (hwhm), $W_{x,y,z} = [20, 16, 16]$ MHz; *biochemical* MCR_{red1}, $\mathbf{g} = [2.242, 2.065, 2.058]$, four identical nitrogen ligands with $a_{iso}(^{14}N) = 30$ MHz, single-crystal Gaussian line widths (hwhm), $W_{x,y,z} = [40, 13, 13]$ MHz; *cryoreduced* MCR_{ox1}, $\mathbf{g} = [2.231, 2.155, 2.155]$, four identical nitrogen ligands with $a_{iso}(^{14}N) = 28$ MHz, $W_{x,y,z} = [13, 15, 15]$ MHz. The other species, which for clarity has no simulation shown, corresponds to MCR_{red1} and can be simulated by $\mathbf{g} = [2.24(1), 2.064, 2.064]$, four identical nitrogen ligands with $a_{iso}(^{14}N) = 28$ MHz, $W_{iso} = 15$ MHz; *biochemical* MCR_{ox1}, $\mathbf{g} = [2.230, 2.167, 2.153]$, four identical nitrogen ligands with $A(^{14}N) = [27, 30, 30]$ MHz, $W_{x,y,z} = [13, 15, 13]$ MHz. For comparison, Albracht et al. had earlier reported the following simulation parameters for MCR_{ox1} in *Mtm* whole cells: $\mathbf{g} = [2.2333, 2.16773, 2.15417]$, four identical nitrogen ligands with $A(^{14}N) = [22, 27, 27]$ MHz, $W_{x,y,z} = [17, 20, 20]$ MHz.[7]

(34) Hyde, J. S.; Froncisz, W. *Annu. Rev. Biophys. Bioeng.* **1982**, *11*, 391−417.

(35) Jaun, B.; Pfaltz, A. *J. Chem. Soc., Chem. Commun.* **1986**, 1327−1329.

(36) Renner, M. W.; Furenlid, L. R.; Stolzenberg, A. M. *J. Am. Chem. Soc.* **1995**, *117*, 293−300.

(37) The inability to resolve ^{14}N hyperfine coupling at $g_{||}$ might reflect residual structural heterogeneity even in relaxed MCR_{red1}, perhaps involving the axial ligand, such as is much more apparent in the original cryoreduced (unrelaxed) species. Studies of model compounds have shown that axial ligands affect the resolution of hyperfine splitting from the macrocyclic ligand.[36]

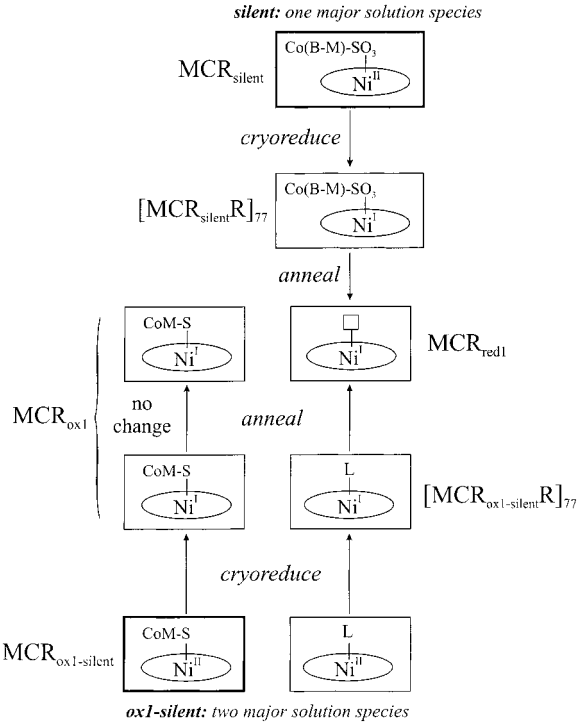

Figure 5. Diagram showing the relations among the crystallographically characterized EPR-silent and EPR-visible forms of MCR, prepared either by cryoreduction or by conventional biochemical methods. The crystallographically determined structures are so indicated by being contained in boldface boxes. The axial ligand in [MCR$_{ox1-silent}$R]$_{77}$ is unknown (indicated simply by L); possible ligands include the same species as in [MCR$_{silent}$]$_{77}$ (the mixed disulfide is abbreviated as Co(B−M)), or a similar moiety, such as the sulfonate group of CH_3S-CoM. We propose that MCR$_{red1}$ has a vacant axial coordination site, as indicated by the empty box. Cryoreduction and annealing of MCR$_{silent}$ yields a single species indistinguishable from authentic MCR$_{red1}$ and this process applied to MCR$_{ox1-silent}$ yields roughly equal amounts of two species that are respectively indistinguishable from MCR$_{ox1}$ and MCR$_{red1}$.

The hyperfine coupling constants determined by simulation of X-band EPR spectra of MCR$_{ox1}$ and of MCR$_{red1}$ each match an average of the individual nitrogen ligand hyperfine couplings ($A_l(^{14}N_i)$, $l = 1-3$, $i = 1-4$) determined by ^{14}N ENDOR of MCR$_{ox1}$ and of MCR$_{red1}$ and related model systems.[15,38] The slight differences in, for example, $A_\perp(^{14}N_i)$ of ∼10% seen by ENDOR [15,38] for MCR$_{red1}$, Ni^{I}OEiBC, and Ni^{I}F$_{430}$ are not resolvable by EPR in our or others' work.[11,35,36] Preliminary ^{14}N ENDOR of cryoreduced MCR$_{red1}$ shows strong similarities with data for biochemically prepared MCR$_{red1}$ and a detailed ENDOR study of all of these MCR species is in progress.

Discussion

X-ray crystallography has provided an exquisite and explicit picture of the two most accessible, but inactive, forms of MCR, namely, MCR$_{silent}$ and MCR$_{ox1-silent}$.[4] Cryoreduction experiments using frozen MCR solutions now provide a structural correlation between structurally characterized EPR-silent Ni(II) forms and the EPR-visible Ni(I) forms, active MCR$_{red1}$ and activateable MCR$_{ox1}$. We discuss this in terms of some of the key questions about the nature of the states presented in Figure 1 and the proposed relationships summarized in Figure 5.

What are the Oxidation States of the EPR-Visible States of MCR? The assignment of Ni(I) to MCR$_{red1}$ is well accepted.[2] Significant biochemical evidence from Thauer's laboratory, however, suggested that the "ox" states of MCR are more oxidized than MCR$_{red1}$, which opened the possibility that the EPR-visible "ox" states could be Ni(III), although the assignment of MCR$_{ox1}$ as Ni(I) also was considered.[2,39] Recently, a combination of EPR/ENDOR spectroscopy, coordination chemistry, and more recent biochemical evidence[8] led us to propose that both MCR$_{ox1}$ and MCR$_{ox2}$ contained Ni(I).[15] Our current results strongly support this proposal. The 77 K γ-irradiation process *reduces* metalloproteins.[16−24] In the experiments reported here, irradiation of EPR-silent Ni(II) forms of MCR yields both MCR$_{red1}$ *and* MCR$_{ox1}$: hence, these two forms can be assigned only as Ni(I) species. Thus, the combination of previous and current spectroscopic and cryoreduction evidence provides overwhelming evidence that *all* EPR-visible forms of MCR are (formally) Ni(I). In the present study, the Ni(I) states are generated from Ni(II) by the mobile electrons generated by γ-irradiation of solvent. Thus far, no chemical reductant has been found that will analogously reduce Ni(II) in either MCR$_{silent}$ or MCR$_{ox1-silent}$ in vitro. However, given that MCR$_{red1}$ and MCR$_{ox1}$ can be isolated via appropriate biochemical procedures, we suggest that a chemical or enzyme-mediated reduction method will eventually be found.

What Are the Ni Coordination Spheres of the EPR-Active, and Functionally Relevant MCR States? Cryoreduction of MCR$_{silent}$ yields as the primary "unrelaxed" product, a species, denoted [MCR$_{silent}$R]$_{77}$, whose EPR spectrum resembles that of MCR$_{red1}$. The X-ray structure of MCR$_{silent}$ defines the Ni axial ligands as the side-chain oxygen of Gln-α147 and a sulfonate oxygen of CoB−SS−CoM;[4] thus, the majority species formed by cryoreduction, [MCR$_{silent}$R]$_{77}$, must contain these two weak axial ligands. Upon annealing to 267 K, this species relaxes to MCR$_{red1}$. This relaxation could involve merely bond adjustments or the detachment of the upper axial sulfonate ligand to give a five-coordinate complex (discussed in more detail below).

The cryoreduction experiments show that frozen-solution MCR$_{ox1-silent}$ actually contains a second major Ni(II) form in addition to MCR$_{ox1-silent}$ itself. We have assigned MCR$_{ox1}$ as the primary product of 77 K cryoreduction of MCR$_{ox1-silent}$. As the MCR$_{ox1}$ is generated without structural relaxation of MCR$_{ox1-silent}$, we conclude that the Ni(I) of MCR$_{ox1}$ has the same distal ligand as the Ni(II) of MCR$_{ox1-silent}$, namely, an axial thiolate ligand from CoM.[4]

The second primary product seen upon cryoreduction of the frozen solution that contains MCR$_{ox1-silent}$, denoted [MCR$_{ox1-silent}$R]$_{77}$, resembles the dominant species formed by cryoreduction of MCR$_{silent}$, denoted [MCR$_{silent}$R]$_{77}$, and both primary species relax upon annealing to form MCR$_{red1}$. This similarity suggests that the EPR-silent parent is the MCR$_{silent}$ state, or equivalent, and that all these species have coordination environments that resemble that of the crystallographically characterized MCR$_{silent}$ state, with the terminal sulfonate group of CoM-SS−CoB as the exogenous axial ligand.

What Occurs during Ti^{III} Citrate-Dependent Activation of MCR$_{ox1}$ to MCR$_{red1}$, Given That Both Oxlike and Redlike Forms of MCR Contain Ni^{I}F$_{430}$, and Thus the Conversion Does Not Involve the Reduction of Ni(III) by Ti(III)? Several spectroscopic techniques show that conversion does involve perturbations of the nickel cofactor. In addition to the shift of $g_\perp$ toward g_e in the EPR spectrum, Ti^{III} citrate-dependent activation causes a 37-nm blue-shift in the UV−visible spectrum.[10] These observations can be explained by the proposal

(38) Telser, J.; Fann, Y.; Renner, M. W.; Fajer, J.; Wang, S.; Zhang, H.; Scott, R. A.; Hoffman, B. M. *J. Am. Chem. Soc.* **1997**, *119*, 733−743.

(39) Rospert, S.; Böcher, R.; Albracht, S. P. J.; Thauer, R. K. *FEBS Lett.* **1991**, *291*, 371−375.

that enzyme activation involves expulsion of the upper axial thiolate ligand in MCR_{ox1} ($CoM-S-Ni^{I}F_{430}$) from the active site, yielding MCR_{red1} where the upper axial coordination site of $Ni^{I}F_{430}$ either is empty or has acquired a relatively weakly coordinating ligand. This would make the Ni(I) of MCR_{red1} accessible for the subsequent formation of the proposed key reaction intermediate, $CH_3-Ni^{III}F_{430}$, through reaction with CH_3S-CoM.[2,40]

This proposal, however, does not suggest a mechanism whereby treatment with Ti^{III} citrate effects removal of the axially coordinated CoM−S(H). It is unclear even as to which properties of Ti^{III} citrate allow this process to occur. Preliminary experiments indicate that the conversion of MCR_{ox1} to MCR_{red1} involves at least one electron; similarly, treating MCR_{ox1} with all components of the activation mixture except Ti(III) results in no activation.[41] Thus, it is apparent that the reducing ability of Ti(III) is necessary. We speculate that the ability of this metal ion to bind sulfur ligands is also important. Perhaps other complexes with reduced, thiophilic metals might also accomplish this activation in vitro. Assuming that a nonmetal-centered reduction is linked to expulsion of the upper axial ligand, what processes are possible? It is likely that the activation process involves sulfur chemistry. The active site contains a thioglcyine residue[4] that could be redox active. Perhaps reduction of this C═S bond to $C-S^{-}$ facilitates expulsion of the upper axial ligand. Activation of MCR_{ox1} to MCR_{red1} results in loss of $^{35}SH^{-}$ (used in the generation of MCR_{ox1}) from radiolabeled protein,[8] Perhaps sodium sulfide acts as a catalyst for the Ti(III)-dependent reduction of the C═S bond of thioglycine.

Are There Relevant Model Compounds? We first consider model compounds for the various redlike species. The crystal structure of MCR_{silent} shows Ni(II) equatorially coordinated by a nearly planar F_{430} tetrahydrocorphinoid macrocycle and weak field, axial oxygen donor ligands: the side-chain oxygen of Gln-α147 and a sulfonate oxygen of CoB−SS−CoM (see Chart 1).[4] Cryoreduction converts MCR_{silent} to the corresponding Ni(I) complex, $[MCR_{silent}R]_{77}$, whose EPR properties (as are those of $[MCR_{ox1-silent}R]_{77}$) are comparable to those of $Ni^{I}F_{430}$ with axial, weak field, oxygen donor ligands, namely, $Ni^{I}F_{430}$ in aqueous solution and $Ni^{I}F_{430}Me_5$ (and Ni^{I}OEiBC) in THF solution (see Table 1).[11,35,36,38] The EPR properties of MCR_{red1} itself are not much different from these as well. This EPR correspondence now includes the ^{14}N hyperfine coupling: MCR_{red1} (and the Ni(I) model compounds[11,35,36]) and MCR_{ox1} *all* exhibit coupling to four equivalent nitrogen ligands with $a_{iso}(^{14}N) \approx 25-30$ MHz. Although we have no *specific* structural basis for the relatively small EPR differences among these redlike species, we note that extensive work on tetraazamacrocyclic complexes of Ni(I) and Ni(II) shows that their electronic properties are quite sensitive to slight changes in type and conformation of axial or equatorial ligand, or both.[42,43]

We can use this model chemistry to speculate on the sources of EPR heterogeneity seen in $[MCR_{silent}R]_{77}$ and $[MCR_{ox1-silent}R]_{77}$, which reflects the conformational distribution present in their parent, Ni(II), forms. Sources of this distribution might include a difference in the upper axial ligand itself; the crystal structure indicates that sulfonate from CoB−SS−CoM occurs in $[MCR_{silent}R]_{77}$, but sulfonate from CH_3S-CoM could conceivably be the ligand in $[MCR_{ox1-silent}R]_{77}$. Even if sulfonate from the mixed disulfide were the upper axial ligand common to all initially produced (unrelaxed) redlike forms, varying conformational forces on this large molecule (see Schemes 1 and 2) could occur. There also may be protein conformational distribution that affects the coordination of the lower axial ligand, Gln-α147 and even protein effects on binding of the side chains of F_{430} that affect the tetrahydrocorphinoid equatorial ligands. Crystallization would "lock in" a single conformation so that these sources of heterogeneity would not be reflected in the structure of MCR_{silent}.

In contrast to the situation with MCR_{red1}, despite numerous beautiful studies of Ni(I) macrocycles with various axial ligands,[42,44−46] there is none with an axially bound thiolate that would therefore provide a model for MCR_{ox1}. We note that thiolato complexes have been reported that model the corresponding Ni(II) parent state, $MCR_{ox1-silent}$, but it is not clear whether such complexes can be reduced to Ni(I).[47,48] We hope that the results presented here will stimulate further synthetic and theoretical work that will shed light on this unusual complex.

In summary, we have (i) confirmed that all EPR-visible forms of MCR contain Ni(I); (ii) for the first time, generated in vitro the enzymatically active MCR_{red1} form and the activateable "ready" MCR_{ox1} form each from "silent" precursors; (iii) combined our results with previous crystallographic data to propose that the exogenous axial ligand in MCR_{ox1} is the thiolate from CoM; (iv) suggested that the exogenous axial ligand of MCR_{red1} may be the terminal sulfonate group of CoM-SS−CoB, as in MCR_{silent}, or a similarly weak ligand.

Acknowledgment. This work was supported by DOE grant DE-FG02-ER20053 (S.W.R.) and NSF grant DMB-9507061 (B.M.H.). We thank Prof. R. K. Thauer (Marburg/Lahn) for communicating unpublished results and for helpful comments.

Supporting Information Available: Four figures (S1−4) showing additional EPR spectra for cryoreduced MCR_{silent} and $MCR_{ox1-silent}$ (PDF). This material is available free of charge via the Internet at http://pubs.acs.org.

JA010428D

(40) Lin, S.-K.; Jaun, B. *Helv. Chim. Acta* **1991**, *74*, 1725−1738.
(41) Horng, Y.-C.; Ragsdale, S. W., unpublished observations.
(42) Lovecchio, F. V.; Gore, E. S.; Busch, D. H. *J. Am. Chem. Soc.* **1974**, *96*, 3109−3118.
(43) Martin, L. Y.; Sperati, C. R.; Busch, D. H. *J. Am. Chem. Soc.* **1977**, *99*, 2968−2981.
(44) Gagné, R. R.; Ingle, D. M. *Inorg. Chem.* **1981**, *20*, 420−425.
(45) Suh, M. P.; Oh, K. Y.; Lee, J. W.; Bae, Y. Y. *J. Am. Chem. Soc.* **1996**, *118*, 777−783.
(46) Chmielewski, P.; Grzeszczuk, M.; Latos-Grazynski, L.; Lisowski, J. *Inorg. Chem.* **1989**, *28*, 3546−3552.
(47) Tada, M.; Masuzawa, Y. *Chem. Commun.* **1997**, 2162−2162.
(48) Ram, M. S.; Riordan, C. G.; Ostrander, R.; Rheingold, A. L. *Inorg. Chem.* **1995**, *34*, 5884−5892.